Thermal expansion properties of Lu_{2-x} $Fe_xMo_3O_{12}$*

Wu Mei-Mei(武梅梅)[a)†], Peng Jie(彭 杰)[b)], Zu Yong(祖 勇)[a)], Liu Rong-Deng(刘荣灯)[a)], Hu Zhong-Bo(胡中波)[c)], Liu Yun-Tao(刘蕴韬)[a)], and Chen Dong-Feng(陈东风)[a)]

[a)] *China Institute of Atomic Energy, Beijing* 102413, *China*

[b)] *Experimental Physics Center, Institute of High Energy Physics, Chinese Academy of Sciences, Beijing* 100049, *China*

[c)] *College of Materials and Photoelectric Technology, Graduate University of Chinese Academy of Sciences, Beijing* 100049, *China*

(Received 21 February 2012; revised manuscript received 15 March 2012)

The structures and thermal expansion properties of $Lu_{2-x}Fe_xMo_3O_{12}$ have been investigated by X-ray diffraction (XRD). XRD patterns at room temperature indicate that compounds $Lu_{2-x}Fe_xMo_3O_{12}$ with $x \leq 1.3$ exhibit an orthorhombic structure with space group *Pnca*; compounds with $x = 1.5$ and 1.7 have a monoclinic structure with space group $P2_1/a$. Studies on thermal expansion properties show that the linear thermal expansion coefficients of orthorhombic phase vary from negative to positive with increasing Fe content. Attempts to make zero thermal expansion materials indicate that zero thermal expansion can be observed in $Lu_{1.3}Fe_{0.7}Mo_3O_{12}$ in the temperature range of 200–400 °C.

Keywords: X-ray diffraction, thermal expansion, crystal structure

PACS: 61.05.cp, 65.40.De **DOI:** 10.1088/1674-1056/21/11/116102

1. Introduction

The family $A_2(MO_4)_3$ (M=Mo and W) has attracted much attention because of their interesting physical and chemical properties. Orthorhombic compounds with a larger cationic radius, like Y^{3+}, Er^{3+}, Tm^{3+}, and Lu^{3+}, exhibit negative thermal expansion, which can be used to adjust the thermal expansion by chemical substitution of the A cation by another trivalent cation.[1−5] In this structure, the A^{3+} exists as an octahedron with six oxygen atoms, where the tungsten or molybdenum ion is surrounded by four oxygen atoms forming a tetrahedra. The A–O–M linkages can accommodate the transverse thermal vibrations necessary for negative thermal expansion. Another interesting feature of this family is their great chemical flexibility, and the radius of A^{3+} may vary from 0.535 Å (Al^{3+}) to 1.06 Å (La^{3+}), which provides a lot of options for making solid solutions to tailor the thermal expansion behaviour.

The correlation between cationic radius and the thermal expansion coefficient of $A_2M_3O_{12}$has been investigated. In $Er_{2-x}Ln_xW_3O_{12}$ (Ln=Ce, Nd, and Sm),[6−8] $Ln_{2-x}Dy_xW_3O_{12}$ (Ln=Er and Y),[9] and $Sc_{2-x}Ga_xW_3O_{12}$[10] systems, the linear thermal expansion coefficient ($\alpha_l = \alpha_V/3$) becomes more negative with the increasing content of larger cations. The α_l of $Er_{2-x}Nd_xW_3O_{12}$ with x=0.1, 0.3, and 0.5 are -6.032×10^{-6}, -6.189×10^{-6}, and -6.280×10^{-6} °C^{-1}, respectively. In $Yb_{2-x}A_xMo_3O_{12}$ (A^{3+}=Cr^{3+} and Al^{3+}) and $Er_{2-x}Fe_xMo_3O_{12}$ systems,[11−13] the α_l changes from negative to positive with the increasing content of smaller cations, even becomes zero by carefully adjusting the Er/Fe ratio in the $Er_{2-x}Fe_xMo_3O_{12}$ system. However, it has been shown that the dependence of α_l on the cation radius is not always straightforward. In $Cr_{2-x}Fe_xMo_3O_{12}$ and $Y_{2-x}Nd_xW_3O_{12}$ systems,[14,15] the cationic substitution leads to the α_l variation in the opposite manner. With the increase of the Nd^{3+} content, the α_l of $Y_{2-x}Nd_xW_3O_{12}$ becomes less negative rather than more negative.

To obtain materials with controllable thermal expansion properties, solid solutions $Lu_{2-x}Fe_xMo_3O_{12}$ have been synthesized and studied by X-ray diffraction (XRD). $Fe_2Mo_3O_{12}$ crystallizes in monoclinic and orthorhombic structures below and above phase transition, respectively, and both phases exhibit positive thermal expansion.[12,16] $Lu_2Mo_3O_{12}$ has an orthorhombic structure and exhibits negative thermal

*Project supported by the National Natural Science Foundation of China (Grant Nos. 10905095, 11105159, and 11075220) and the National Basic Research Program of China (Grant No. 2010CB833101).

†Corresponding author. E-mail: mmwu@ciae.ac.cn

© 2012 Chinese Physical Society and IOP Publishing Ltd

expansion.[17] Therefore, it is possible to make thermal expansion coefficients controllable by adjusting the Lu/Fe ratio. We herein will report our work on the synthesis, structure, and thermal expansion behaviour of solid solution $Lu_{2-x}Fe_xMo_3O_{12}$.

2. Experiment

Polycrystalline samples $Lu_{2-x}Fe_xMo_3O_{12}$ (x = 0.3, 0.5, 0.7, 1.0, 1.3, 1.5, and 1.7) were synthesized by the conventional solid-state reaction from the corresponding oxides Lu_2O_3 (purity 99.9%), Fe_2O_3 (purity 99.9%), and MoO_3 (purity $\geq$ 99.0%). Stoichiometric amount of raw materials were thoroughly mixed and heated at 700–800 °C in aluminum crucibles for 48 h with an intermediate regrinding, and then slowly cooled to room temperature in the furnace.

Room-temperature XRD data were recorded on a Bruker D8 ADVANCE with DAVINCI design X-ray diffraction machine with Cu K_α radiation at China Institute of Atomic Energy. Variable-temperature XRD data were collected for $Lu_{2-x}Fe_xMo_3O_{12}$ (x = 0.3, 0.7, and 1.0) at 200, 300, 400, 500, 600, 700, and 800 °C, and for $Lu_{0.5}Fe_{1.5}Mo_3O_{12}$ at 25, 250, 400, 500, 600, 700, and 800 °C to elucidate their thermal expansion properties, on a PAN X'Pert PRO MPD with Cu K_α radiation at Beijing Normal University. The well-ground sample was mounted on a Pt–Rh strip, which serves as a sample holder and heating element. The heating speed was 20 °C min and each temperature was kept for 5 min before the data was collected. Rietveld refinements of the XRD data were performed using the program Fullprof.[18]

Thermogravimetric (TG) analysis of $Lu_{2-x}Fe_xMo_3O_{12}$ (x = 0.3 and 0.5) were performed under nitrogen atmosphere from room temperature to 400 °C using a TA instrument SDT Q600 thermal analyzer in Peking University. The heating rate was 10 °C/min, and Al_2O_3 powder was used as the reference material.

3. Results and discussion

3.1. XRD characterization

The phase purity of the prepared samples $Lu_{2-x}Fe_xMo_3O_{12}$ is confirmed by XRD, and the diffraction pattern of the newly synthesized compound at room temperature are depicted in Fig. 1(a) . There are no additional peaks from impurities in the whole composition range. Samples $Lu_{2-x}Fe_xMo_3O_{12}$ with $x \leq 1.3$ crystallize in $Lu_2Mo_3O_{12}$-type orthorhombic symmetry with space group *Pnca*. The diffraction patterns for $x = 1.5$ and 1.7 can be indexed in monoclinical symmetry with space group $P2_1/a$. The presence or absence of the diffraction peak at $2\theta \approx 26.3°$ (as indicated by M in Fig. 1(a)) indicates the existence of a monoclinic or orthorhombic structure. Orthorhombic compounds are easily hygroscopic, which partially destroys the framework of the original structure and results in some amorphous phase.[3,19] A high background noise and fewer diffraction peaks can be seen in the pattern of the compound after being exposed for several days in air (see Fig. 1(b)).

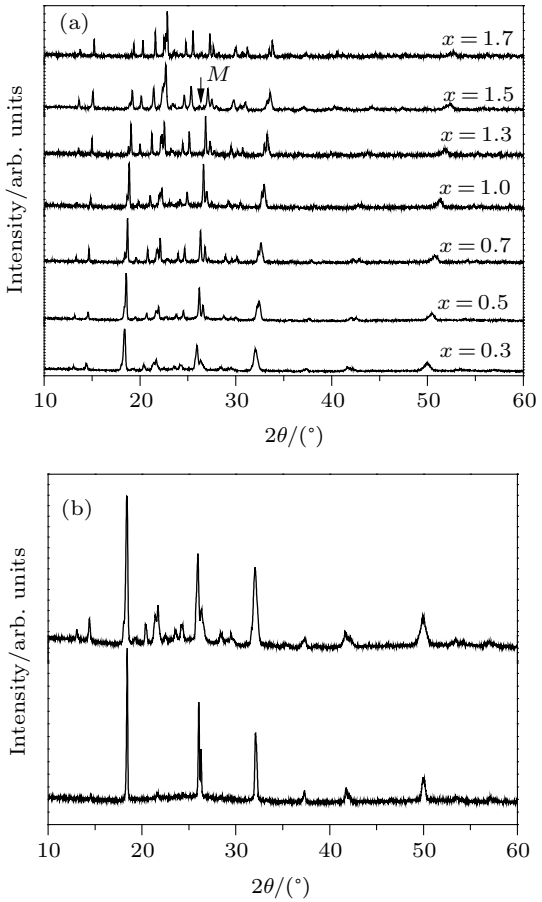


Fig. 1. (a) XRD patterns of the newly synthesized compound at room temperature. (b) Upper line: the newly synthesized compound of $Lu_{1.7}Fe_{0.3}Mo_3O_{12}$; lower line: compound exposed in air for several days.

For orthorhombic and monoclinic phases, the initial structure parameters used in the Rietveld refinements were taken from those reported for $Sc_2Mo_3O_{12}$[20] and $Fe_2Mo_3O_{12}$.[21] The lattice parameters and unit cell volumes of partial $Lu_{2-x}Fe_xMo_3O_{12}$ were summarized in Table 1. The lattice parameters a, b, c, and unit cell volume V decrease with increasing Fe^{3+} content, due to the smaller ionic radius of Fe^{3+} (0.64 Å) compared with that of Lu^{3+} (0.85 Å).

Table 1. Lattice parameters of $Lu_{2-x}Fe_xMo_3O_{12}$ ($x = 0.3$, 0.7, and 1.0) at 200 °C and $Lu_{2-x}Fe_xMo_3O_{12}$ ($x = 1.5$ and 1.7) at room temperature.

Compound	a/Å	b/Å	c/Å	β/(°)	V/Å^3
$x = 0.3$	9.8080(5)	13.5842(6)	9.7381(4)	–	1297.5(1)
$x = 0.7$	9.6908(3)	13.3548(4)	9.5917(3)	–	1241.4(1)
$x = 1.0$	9.5961(4)	13.2174(5)	9.4950(4)	–	1204.3(1)
$x = 1.5$	15.9515(8)	9.3716(4)	18.4890(8)	125.620(3)	2246.8(2)
$x = 1.7$	15.8408(3)	9.3210(1)	18.3808(3)	125.379(1)	2212.8(1)

3.2. Thermogravimetric analysis

TG curves (see Fig. 2) of $Lu_{2-x}Fe_xMo_3O_{12}$ (x=0.3 and 0.5) indicate that the orthorhombic samples are highly hygroscopic at room temperature, which has been observed in the isostructural compound $A_2M_3O_{12}$ (M=W and Mo).[17,21–23] We can observe that the weight loss occurs between 50 and 135 °C. The TG curves have two different inclinations that correspond to a two-step behaviour in the waterlosing process, which change the slope at around 95.5 and 102.9 °C for $x = 0.3$ and 0.5, respectively. The water loss in isostructural molybdates occurs from room temperature to 150 °C in $Ln_2Mo_3O_{12}$ (Ln=Y, Er, Yb, or Lu),[17] similar to our experimental results. The weight loss of $Lu_{2-x}Fe_xMo_3O_{12}$ ($x = 0.3$ and 0.5) is 6.6% and 5.0%, and the corresponding water molecule number per formula unit is 3.1 and 2.3, respectively.

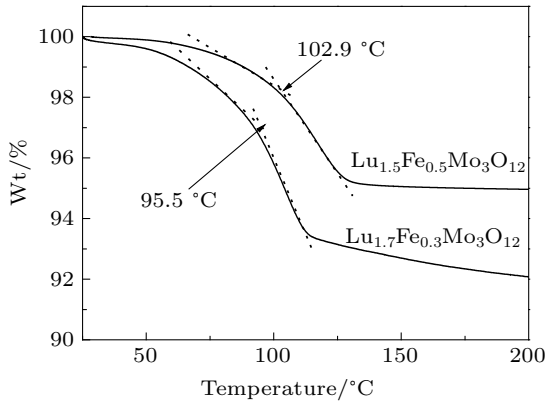


Fig. 2. TG curves of $Lu_{2-x}Fe_xMo_3O_{12}$ ($x = 0.3$ and 0.5).

Obviously, the partial substitution of Fe^{3+} for Lu^{3+} prevents the water molecule entering into the framework of the crystal structure. It could be explained that the structural voids for water accommodation become smaller due to the increasing Fe^{3+} content. The effect of water molecules on the thermal expansion property has been discussed in some tungstates and molybdates.[23] The presence of water molecules would prevent negative thermal expansion. Only after the complete removal of water molecules, these compounds can exhibit negative thermal expansion. Therefore, the data above 200 °C were used to study the thermal expansion properties for orthorhombic compounds.

3.3. High-temperature X-ray diffraction studies

High-temperature X-ray diffraction data indicate that $Lu_{2-x}Fe_xMo_3O_{12}$ ($x = 0.3$ and 1.0) remains the orthorhombic structure in the temperature range of 200–800 °C. Structural refinements were carried out for all samples using data obtained at various temperatures. To examine the quality of the refinements, the diffraction patterns of $Lu_{1.7}Fe_{0.3}Mo_3O_{12}$ at 200 and 800 °C are shown in Fig. 3. The agreement between the observed and calculated intensities is excellent, and it is worthwhile to note that in this case there is no evidence of the presence of phase transition.

The variations of cell parameters and volumes of $Lu_{2-x}Fe_xMo_3O_{12}$ ($x = 0.3$ and 1.0) as functions of the temperature are plotted in Figs. 4(a)–4(d). The axial and linear coefficients of thermal expansion (CTEs) obtained from these data are tabulated in Table 2. The CTEs of $Lu_2Mo_3O_{12}$ have also been given for comparison. $Lu_{1.7}Fe_{0.3}Mo_3O_{12}$ shows thermal contraction along the a and c axes, while the b axis exhibits near zero thermal expansion in the whole temperature range. This leads to an overall volume contraction with $\alpha_l = -5.59 \times 10^{-6}$ °C^{-1}. $LuFeMo_3O_{12}$ shows a slight contraction along the a and c axes, but the strong expansion of the b axis results in a low positive linear thermal expansion coefficient ($\alpha_l = 0.987 \times 10^{-6}$ °C^{-1}).

$Lu_{0.5}Fe_{1.5}Mo_3O_{12}$ crystallizes in monoclinic structure at low temperature, and then transforms to the orthorhombic structure at and above 400 °C. Figures 4(e)–4(i) show the cell parameters of $Lu_{0.5}Fe_{1.5}Mo_3O_{12}$ with the rising temperature. Unit cell parameters a, b, and c in the monoclinic phase

all exhibit positive thermal expansion. For the orthorhombic phase, the cell parameters b and c show positive thermal expansion, and the a axis shows negative thermal expansion. The axial and linear coefficients of thermal expansion for the orthorhombic phase are also listed in Table 2.

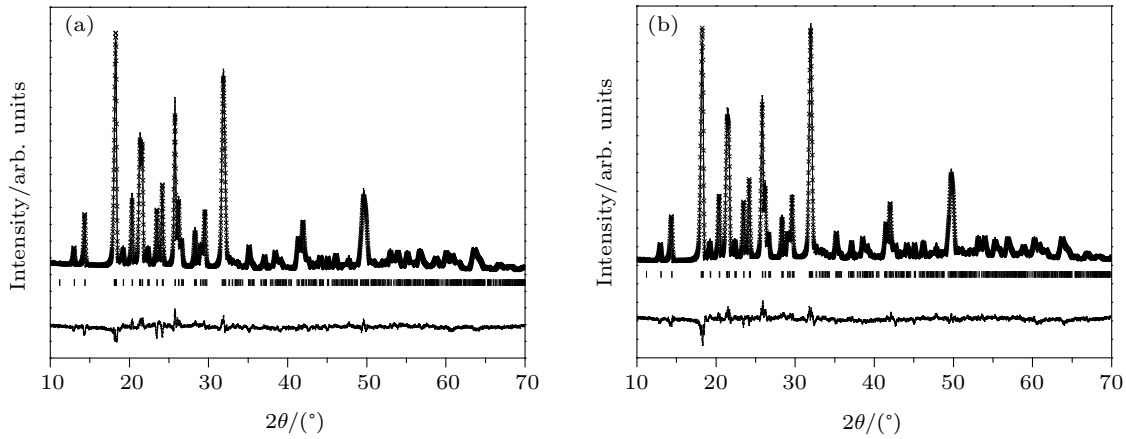


Fig. 3. Rietveld refinement of XRD pattern of $Lu_{1.7}Fe_{0.3}Mo_3O_{12}$ at (a) 200 °C ($R_p = 4.11\%$, $R_{wp} = 5.12\%$) and (b) 800 °C ($R_p = 4.12\%$, $R_{wp} = 5.22\%$). Observed (×), calculated (solid line), Bragg position (|), and difference plots (lowest trace) are shown.

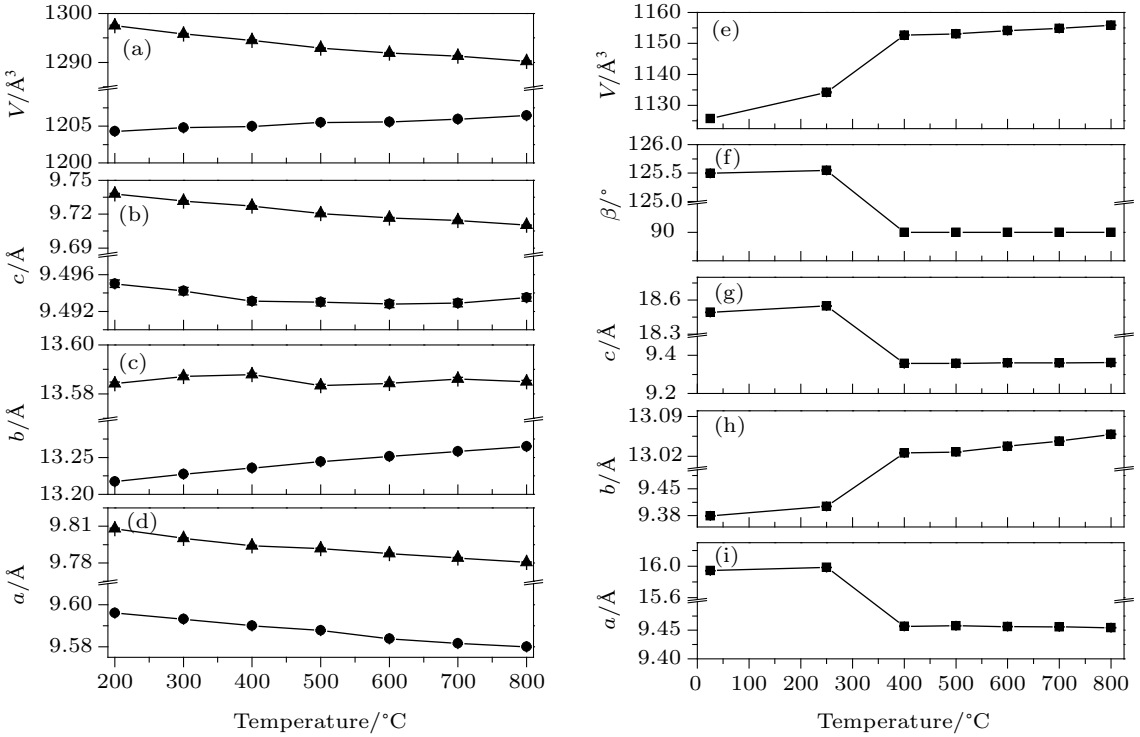


Fig. 4. Thermal evolution of cell parameters of (a–d) $Lu_{2-x}Fe_xMo_3O_{12}$ ($x = 0.3$ (▲) and 1.0 (●)) and (e–i) $Lu_{0.5}Fe_{1.5}Mo_3O_{12}$. The cell volume of the monoclinic phase has been halved for comparison with the orthorhombic one.

Table 2. Coefficients of thermal expansion for $Lu_{2-x}Fe_xMo_3O_{12}$.

	$\alpha_a/10^{-6}$ °C^{-1}	$\alpha_b/10^{-6}$ °C^{-1}	$\alpha_c/10^{-6}$ °C^{-1}	$\alpha_l/10^{-6}$ °C^{-1}
$x = 0.0$ (200–800 °C)[3]	−8.88	−1.23	−6.62	−5.59
$x = 0.3$ (200–800 °C)	−4.690	0.123	−4.775	−3.126
$x = 1.0$ (200–800 °C)	−2.796	6.015	−0.263	0.987
$x = 1.5$ (400–800 °C)	−0.441	4.222	0.819	2.313

The orthorhombic $Fe_2Mo_3O_{12}$ and $Lu_2Mo_3O_{12}$ have the opposite thermal expansion properties. As a result, the CTEs of compounds $Lu_{2-x}Fe_xMo_3O_{12}$ can be controlled by adjusting the Fe/Lu ratio. Figure 5 shows the CTEs of samples with $x = 0.0$, 0.3, 1.0, and 1.5. The lines in this figure imply that thermal expansion coefficients are almost linearly related to x. From this figure, we can speculate that zero thermal expansion may be realized at around $x = 0.7$, thus temperature-dependence XRD data were also collected for sample $Lu_{1.3}Fe_{0.7}Mo_3O_{12}$ in the same manner.

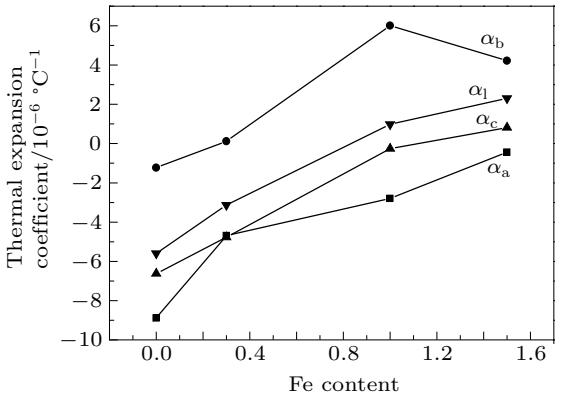


Fig. 5. Thermal expansion coefficients versus Fe content (x).

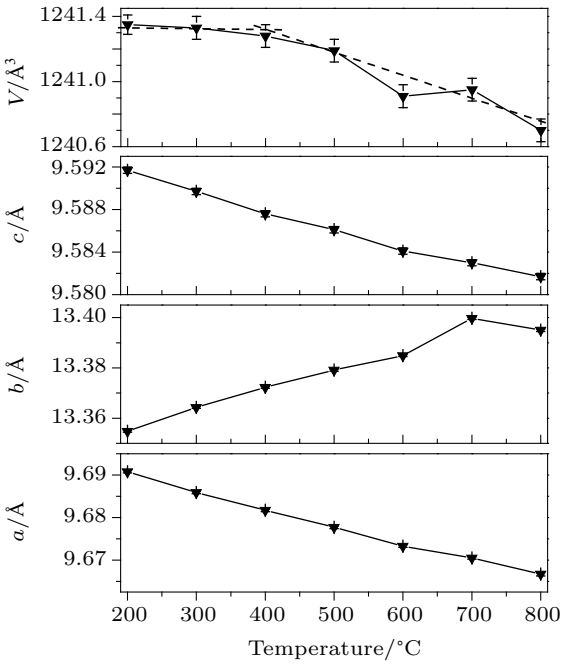


Fig. 6. Cell parameters a, b, and c, and V of $Lu_{1.3}Fe_{0.7}Mo_3O_{12}$ versus temperature.

Figure 6 shows the variations of cell parameters a, b, and c, and unit cell volume V of $Lu_{1.3}Fe_{0.7}Mo_3O_{12}$ with the rising temperature. The lattice parameters a and c contract with the increasing temperature, and b expands in the temperature range of 200–700 °C. It is worth pointing out that the α_l of $Lu_{1.3}Fe_{0.7}Mo_3O_{12}$ is zero in the temperature range of 200–400 °C, if the standard deviation is considered. It exhibits near zero α_l of -0.389×10^{-6} °C^{-1} in the higher temperature range.

The crystal structure of orthorhombic $Lu_{2-x}Fe_xMo_3O_{12}$ is composed of a corner-sharing network of $Lu(Fe)O_6$ octahedra and MoO_4 tetrahedra, where each oxygen atom bridges one Lu (Fe) and one Mo atom. Negative thermal expansion can be found in orthorhombic $A_2M_3O_{12}$ with larger ionic size A^{3+}, such as Y^{3+}, Er^{3+}, and Lu^{3+}. The mechanism of negative thermal expansion in the $A_2M_3O_{12}$ family is attributed to the rocking motion of polyhedra based on the correlated transverse thermal vibration of oxygen perpendicular to A–O–M linkages. However, the rocking motions occur only when the polyhedra can undergo some slight distortion.[1,24] The distortions of polyhedra occur easily in large polyhedra where the repulsive oxygen–oxygen interactions are minimized. Rigid polyhedra will prohibit the rocking motion and the negative thermal expansion. The replacement of Fe for Lu results in the decrease of the average size of the central cation and the volume of $Lu(Fe)O_6$ polyhedra. Thus the oxygen–oxygen repulsive interaction in polyhedral is enhanced, which leads to the higher rigidity of the polyhedra. As a result, $Lu_{1.7}Fe_{0.3}Mo_3O_{12}$ exhibits negative thermal expansion, while $LuFeMo_3O_{12}$ and compounds with a higher Fe content possess positive thermal expansion. The linear thermal expansion coefficient changes from negative to positive with increasing Fe^{3+} content, even becomes zero when $x = 0.7$ in the 200–400 °C temperature range.

4. Conclusions

Solid solutions $Lu_{2-x}Fe_xMo_3O_{12}$ have been prepared successfully and characterized by X-ray diffraction. All the compounds are single phase, and the cell parameters decrease with increasing Fe content. TG analysis shows that orthorhombic $Lu_{2-x}Fe_xMo_3O_{12}$ ($x = 0.3$ and 0.5) is highly hygroscopic at room temperature and loses water at a temperature of between 50 and 135 °C. The linear thermal expansion coefficient for orthorhombic $Lu_{2-x}Fe_xMo_3O_{12}$ ($x = 0.3$, 1.0, and 1.5) is -3.126×10^{-6}, 0.987×10^{-6}, and 2.313×10^{-6} °C^{-1}, respectively. The zero thermal expansion coefficient of $Lu_{1.3}Fe_{0.7}Mo_3O_{12}$ is observed

in the temperature range of 200–400 °C, and near zero thermal expansion coefficient of -0.389×10^{-6} °C^{-1} is observed in the higher temperature range of 400–800 °C.

References

[1] Forster P M, Yokochi A and Sleight A W 1998 *J. Solid State Chem.* **140** 157

[2] Sleight A W 1998 *Annu. Rev. Mater. Sci.* **28** 29

[3] Evans J S O, Mary T A and Sleight A W 1997 *J. Solid State Chem.* **133** 580

[4] Evans J S O, Mary T A and Sleight A W 1997 *Physica* B **241** 311

[5] Evans J S O 1999 *J. Chem. Soc., Dalton Trans.* 3317

[6] Wu M M, Cheng Y Z, Peng J, Xiao X L, Chen D F, Kiyanagi R, Fieramosca J S, Short S, Jorgensen J and Hu Z B 2007 *Mater. Res. Bull.* **42** 2090

[7] Wu M M, Peng J, Cheng Y Z, Xiao X L, Hao Y M and Hu Z B 2007 *Mater. Sci. Eng.* B **137** 144

[8] Wu M M, Peng J, Cheng Y Z, Wang H, Yu Z X, Chen D F and Hu Z B 2006 *Solid State Sci.* **8** 665

[9] Xiao X L, Peng J, Wu M M, Cheng Y Z, Chen D F and Hu Z B 2008 *J. Alloy. Compd.* **465** 556

[10] Liu F S, Chen X P, Xie H X, Ao W Q and Li J Q 2010 *Acta Phys. Sin.* **59** 3350 (in Chinese)

[11] Wu M M, Xiao X L, Hu Z B, Liu Y T and Chen D F 2009 *Solid State Sci.* **11** 325

[12] Li Q J, Yuan B H, Song W B, Liang E J and Yuan B 2012 *Chin. Phys.* B **21** 046501

[13] Cheng Y Z, Wu M M, Peng J, Xiao X L, Li Z X, Hu Z B, Kiyanagi R, Fieramosca J S, Short S and Jorgensen J 2007 *Solid State Sci.* **9** 693

[14] Ari M, Jardim P M, Marinkovic B A, Rizzo F and Ferreira F F 2008 *J. Solid State Chem.* **181** 1472

[15] Peng J, Wu M M, Wang H, Hao Y M, Hu Z, Yu Z X, Chen D F, Kiyanagi R, Fieramosca J S, Short S and Jorgensen J 2008 *J. Alloy. Compd.* **453** 49

[16] Tyagi A K, Achary S N and Mathews M D 2002 *J. Alloy. Compd.* **339** 207

[17] Sumithra S and Umarji A M 2006 *Solid State Sci.* **8** 1453

[18] Rodriguez-Carjaval J 2005 An Introduction to the Program Laboratoire Leon Brillouin (CEA-CNRS) France

[19] Marinkovic B A, Jardim P M, Avillez R R and Rizzo F 2005 *Solid State Sci.* **7** 1377

[20] Evans J S O and Mary T A 2000 *Inter. J. Inorg. Mater.* **2** 143

[21] Chen H Y 1979 *Mater. Res. Bull.* **14** 1583

[22] Sumithra S and Umarji A M 2004 *Solid State Sci.* **6** 1313

[23] Sumithra S and Umarji A M 2005 *Mater. Res. Bull.* **40** 167

[24] Forster P M and Sleight A W 1999 *Int. J. Inorg. Mater.* **1** 123